

## Electronic Supplementary Information

### Tunable light emission from co-assembled structures of benzothiadiazole molecules

Kaushik Balakrishnan,<sup>†\*</sup> Wei-Liang Hsu,<sup>†</sup> Shuntaro Mataka<sup>‡</sup> and Stanley Pau<sup>†\*</sup>

<sup>†</sup>College of Optical Sciences, The University of Arizona, Tucson, AZ 85721, and <sup>‡</sup>Institute for Materials Chemistry and Engineering, Kyushu University, 6-1 Kasuga-koh-en, Kasuga-shi, Fukuoka 816-8580, Japan

#### Table of Contents

Experimental .....	2
Supporting Figures .....	4
Supporting Information Reference.....	11

## Experimental

The solvents (ethanol and chloroform) used for the preparation of co-assemblies were purchased from commercial suppliers and used as received.

### Synthesis of **1** and **2**

The synthesis and characterization of **1** and **2** are well described in prior works.<sup>1</sup>

### Protocols for self-assembly and co-assemblies of **1** and **2**

In our previous works, we have employed a slow-phase transfer method to produce extremely large microtubules of **1**. However, to ensure compatibility of the two components and prepare well-defined structures we note that simple solvent exchange procedures employed before were ineffective and produced ill defined morphology. To this end, a new protocol has been advanced to produce well-defined morphology. Certain composition of **1** and **2** were prepared in chloroform solvent as stocks and appropriately diluted to prepare 33  $\mu\text{M}$  total concentration. The seven different compositions chosen were as follows **1**<sub>100%</sub>, **1**<sub>90%</sub> + **2**<sub>10%</sub>, **1**<sub>75%</sub> + **2**<sub>25%</sub>, **1**<sub>50%</sub> + **2**<sub>50%</sub>, **1**<sub>25%</sub> + **2**<sub>75%</sub>, **1**<sub>10%</sub> + **2**<sub>90%</sub>, **2**<sub>100%</sub>. These solutions are pictorially shown in **Fig. S1**. Once the specific compositions were prepared, a fixed amount ( $\sim 0.5$ -1 mL) of the solution was transferred to a small testing tube and chloroform was evaporated by immersing in a water bath (set at 70 °C). Following this, the tubes were allowed to stabilize at room temperature. To achieve controlled assemblies, 1 mL of ethanol and 100  $\mu\text{L}$  of chloroform were added and the solution was re-immersed in the water bath to ensure complete dissolution. The complete dissolution can be observed under UV-light. Small floating aggregates that are clearly notable at the early stages of heating have dissolved completely and uniform emission under UV-photoexcitation from solution is evident. Typically, this step takes  $\sim 5$  minutes. The solution is then allowed to cool to room temperature and then left undisturbed overnight. It should be ensured that no precipitates are visible at this stage. After  $\sim 30$  minutes of reaching room temperature, aggregates are apparent. UV-excitation using hand held lamp indicates a uniform color for each of the specific composition. These aggregates are then characterized using a range of spectroscopic and microscopic techniques. This method is therefore well suited for controlling the morphology particularly in co-assemblies as it allows for strategic incorporation of the two components and does not promote phase-separation as noted for other methods such as solvent exchange, used previously to yield ultra-long microtubules from **1**.

### Characterization

UV-Visible spectroscopy was performed using Cary 5000. Appropriate sample holders were used to measure the solution and solid-state spectra. Fluorescence spectral measurements were acquired using a PTI instrument fitted with liquid and solid state cells. SEM was performed using FEI quanta microscope operated at a working voltage of 30 kV. The samples were lightly sputtered by gold before morphological inspection. The self-assembled structures were cast on Si surface and allowed to dry before gold sputtering and SEM analysis. Image corrections and analysis was performed using Photoshop CS6 and Image J.

Fluorescence microscopy was carried out using Nikon Eclipse scope with different excitation filters suitable for identifying the strategic emission from individual and co-assembled structures. The aggregates were cast on cover glass slides and mounted on standard microscope slides for evaluation using different objectives and filters. The images were acquired using

different exposure times to optimize the measurement of emitted light. The three filters that were used are designated as f1, f2 and f3. The details of the filters are shown in **Table 1**.

**Table 1:** The various filters used in the collection of emission from the co-assembled structures.

Filter	Excitation (nm)/ band pass (nm)	Dichroic (nm)	Emission (nm)
f1	480/ 30	505	535 / 40
f2	540 / 25	565	620 / 60
f3	600 / 65	685	690 / 70

It can be noted from the choice of filters and the spectral emissions that f1 is well suited for characterizing the emission from **1**, while f2 and f3 are well suited towards identifying regions of co-assembled structures and pure **2**. Thus, these three filters along with the spectral measurements allow us to detail the characteristic emission from the co-assembled structures and the co-localization of the molecular entities **1** and **2** within the co-assembled structures.

**Notes:**

**N1:** Except for **C2**, where small amounts of pure **1** aggregates could be noted for both fluorescence microscopic and spectroscopic (see **Fig. S11**) analysis no phase separation was notable for other composition in **C2**. Even in **C2**, most of the emission was from the co-assembled structures. This is because of the rich level of composition of **1** in respect to **2**. Furthermore, the emission from **C3** is very close to that of **C2**. The main reason for including **C2** as a valuable marker composition in our case is to signify the subtle balance of molecular interactions between **1** and **2** indicating that even at very low compositions, the co-assembly can lead to rich possibility for tuning light emission by adjusting the composition.

## Supporting Figures

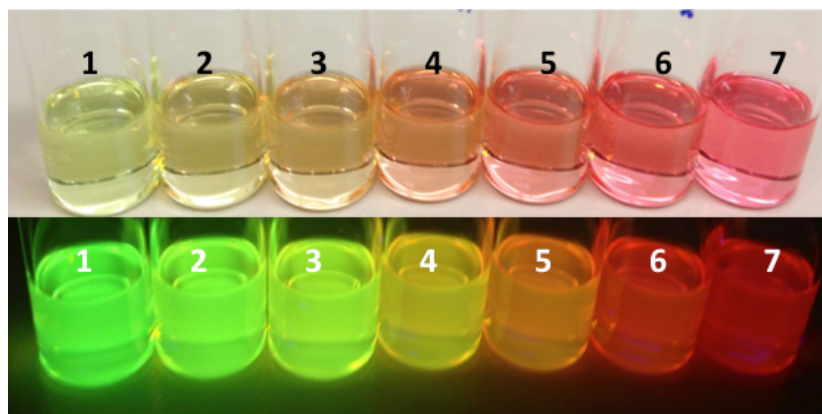


**Figure S1.** Chloroform solutions of C1-C7. Top panel shows the color of solution under normal conditions while the bottom panel shows the strong fluorescence upon UV-illumination.

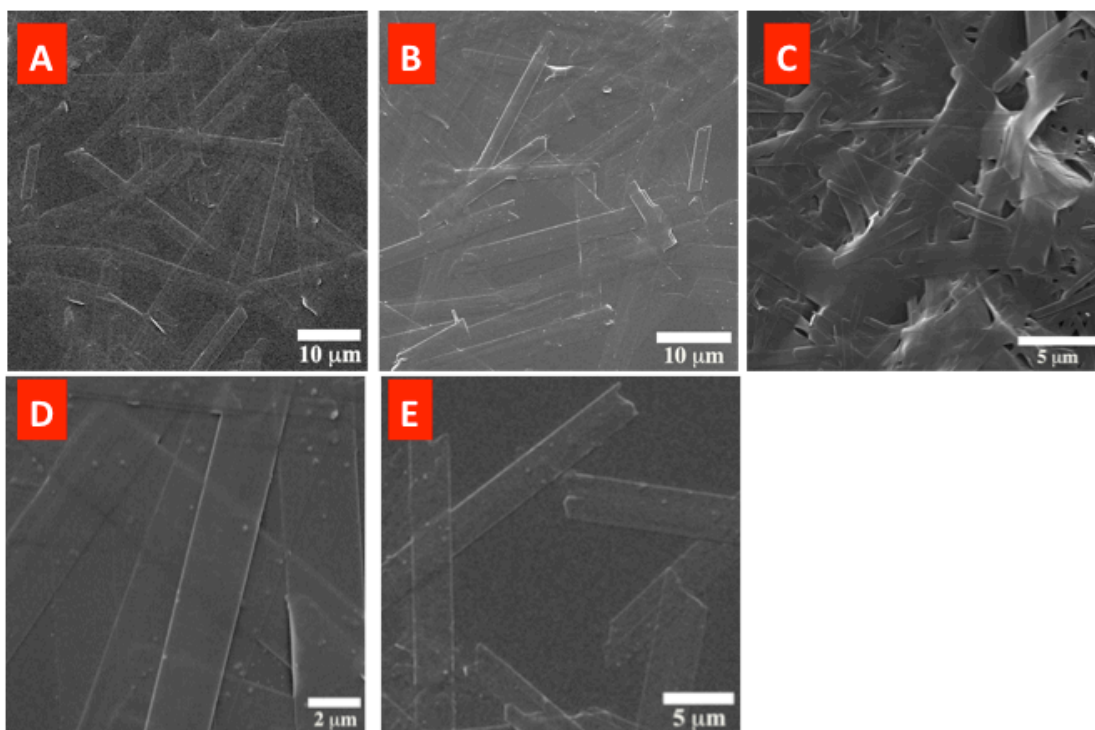


**Figure S2.** More SEM images for the assemblies from pure 1 (C1).

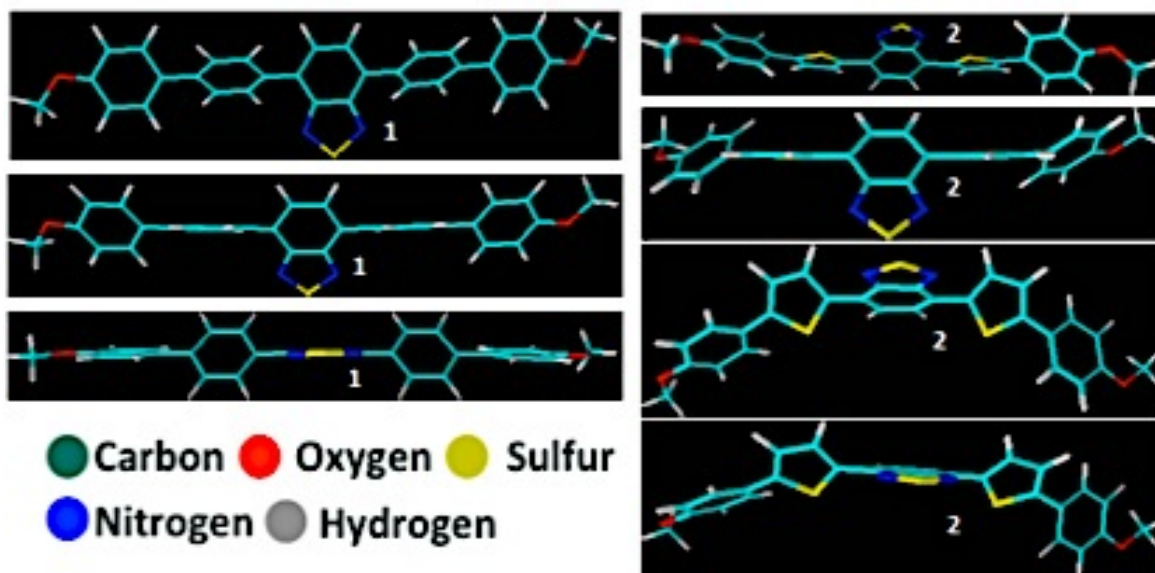


**Figure S3.** Geometry optimization of **1** and **2** using MMFF94 (Chemdraw 3D, 12.0). For **1** the overall planarity of the molecule is apparent while for **2** there is considerable distortion. The local molecular distortion within **1** and global distortion of **2** lead to strong emission possibilities, given the manner in which they assemble.

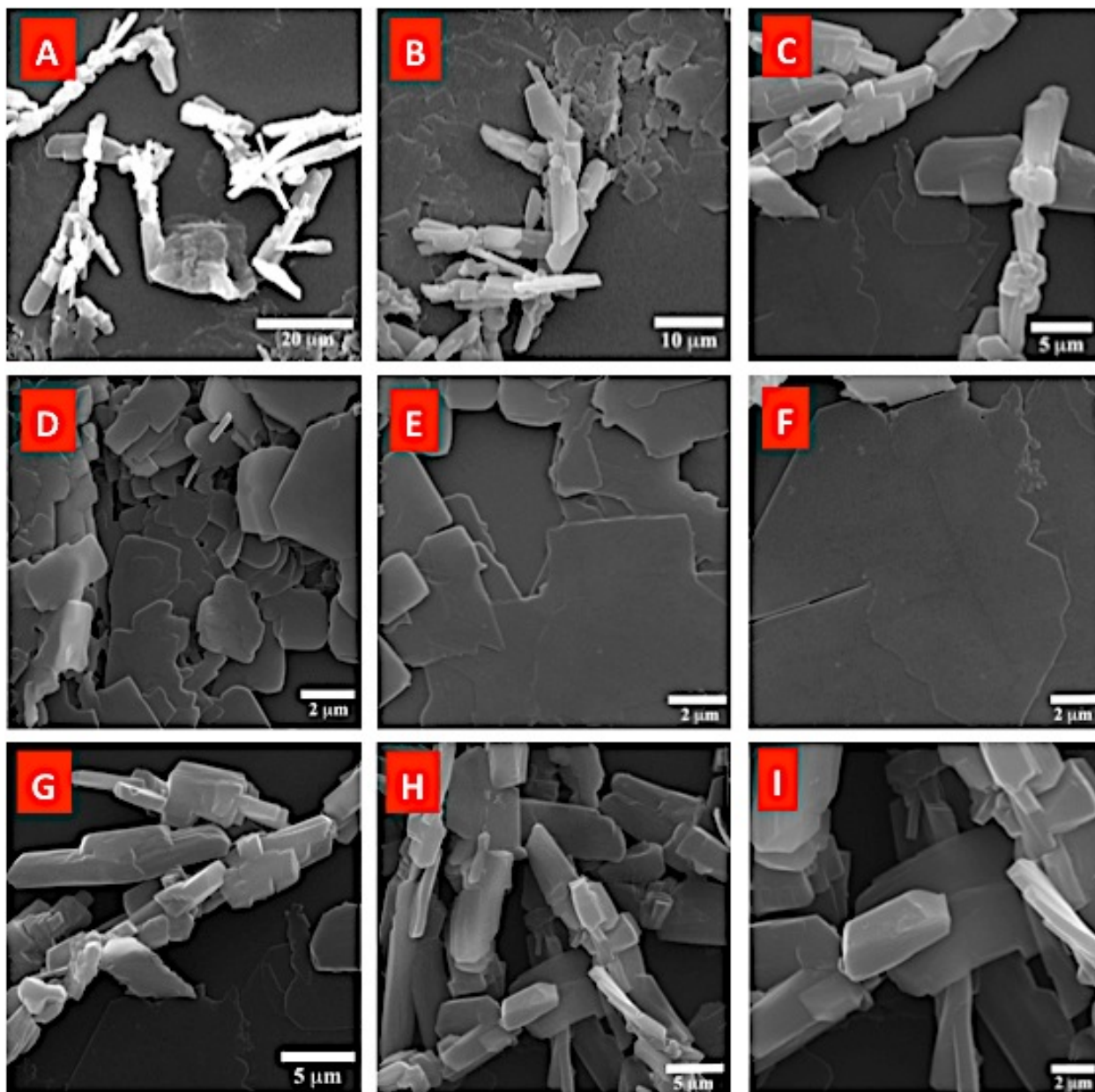


**Figure S4.** 3D crystallites and 2D sheet like morphology produced using slow cooling of ethanol/chloroform solution of **2** (C7).

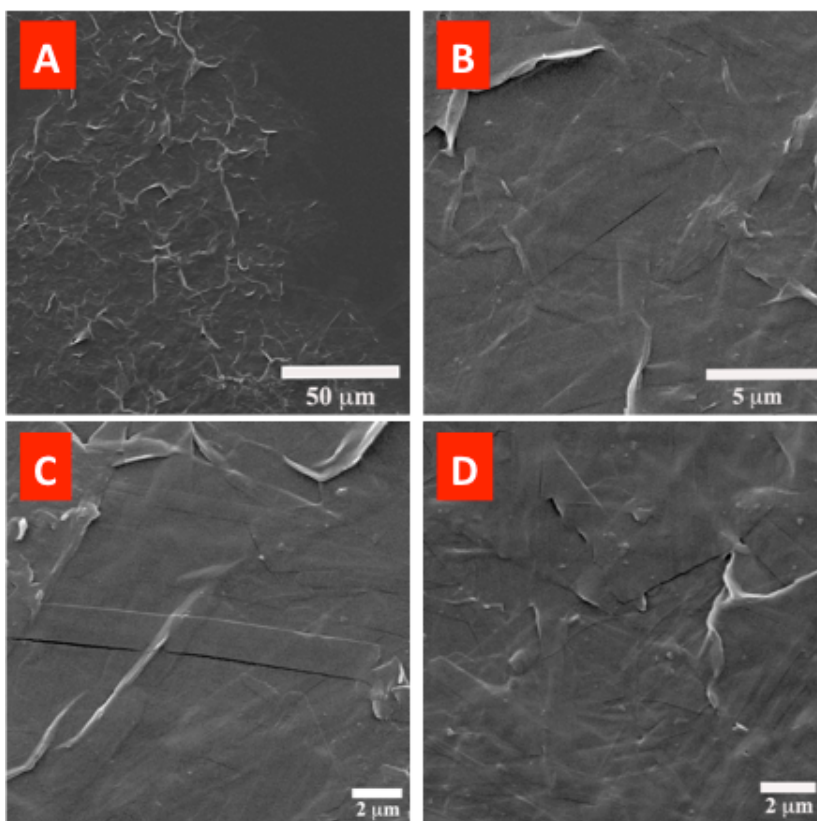


**Figure S5.** Ribbon like morphology produced using slow cooling of ethanol/chloroform solution of composition **C2**.

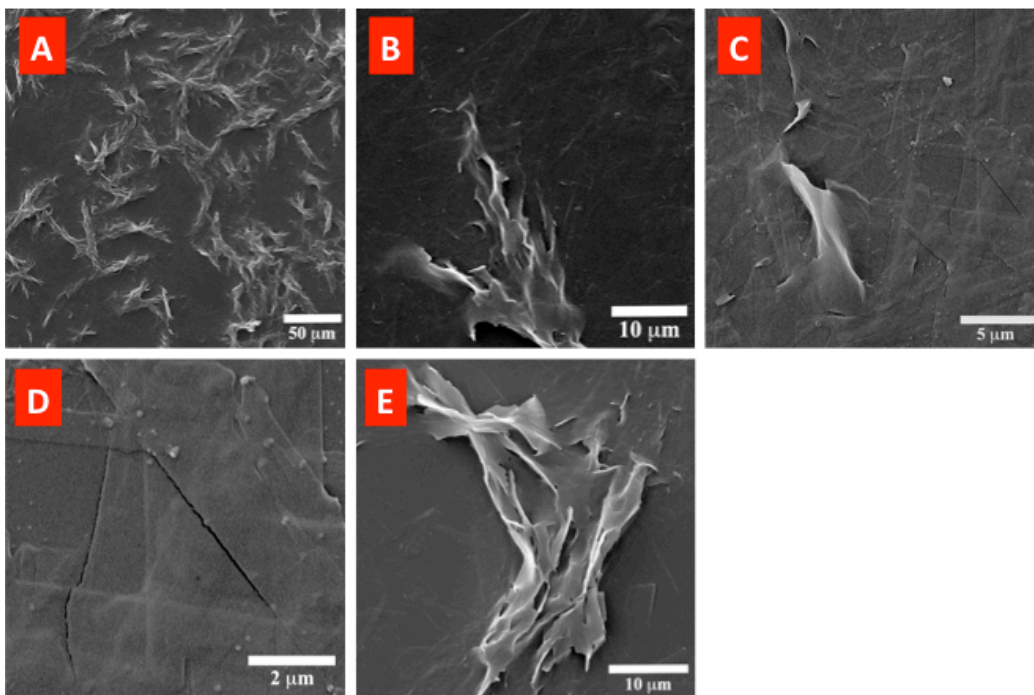


**Figure S6.** Ribbon like morphology produced using slow cooling of ethanol/chloroform solution of **C3**.

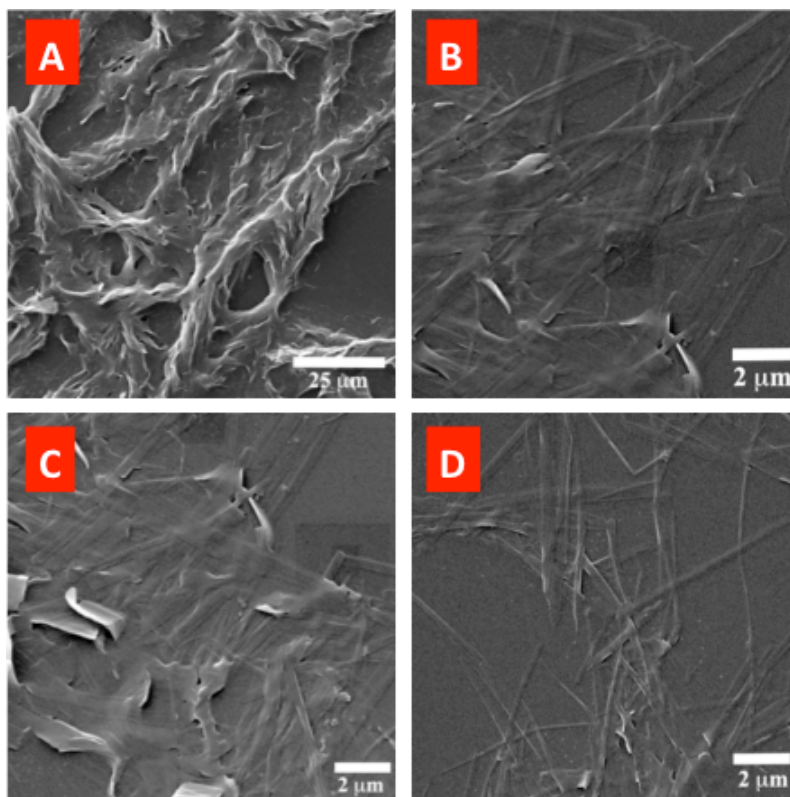


**Figure S7.** Ribbon like morphology produced using slow cooling of ethanol/chloroform solution of **C4**.

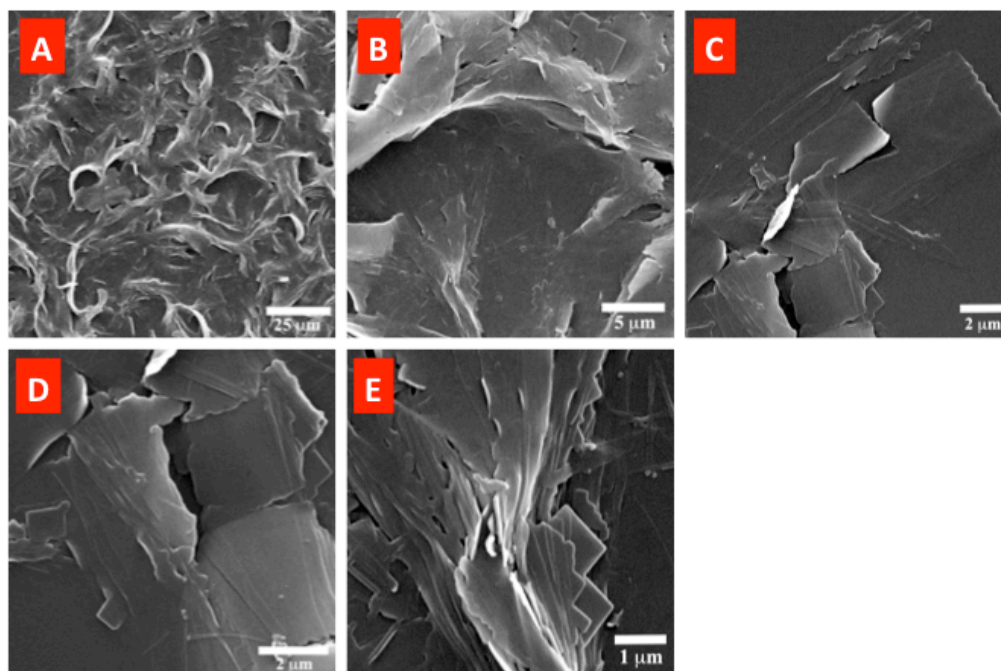


**Figure S8.** Sheet like morphology produced using slow cooling of ethanol/chloroform solution of **C5**.



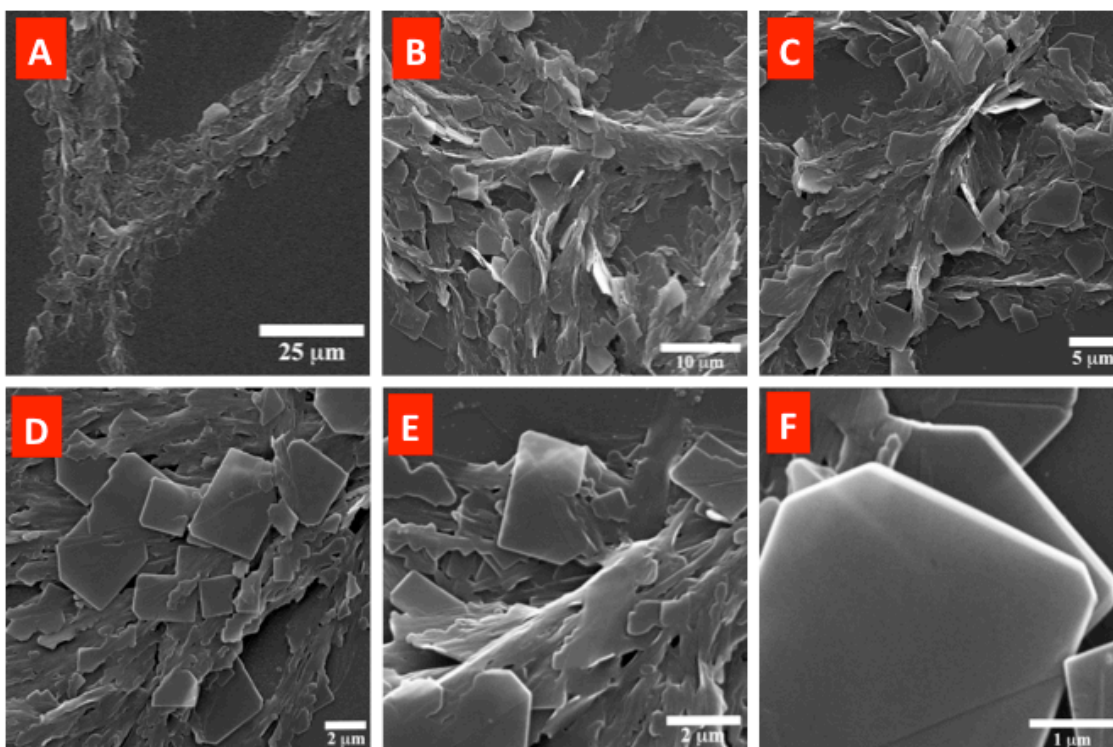


**Figure S9.** Sheet and tile like morphology produced using slow cooling of ethanol/chloroform solution of C6.

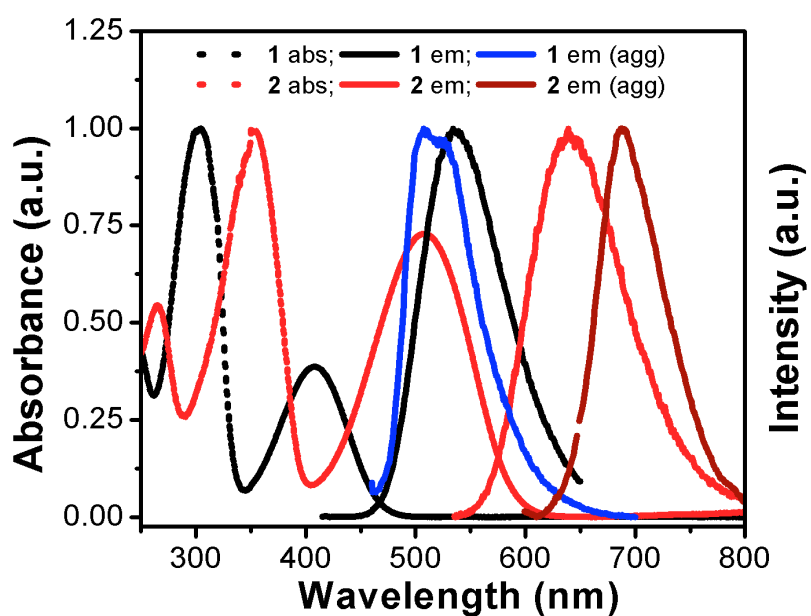


**Figure S10.** The solid-state emission from pure components along with absorption and emission from the molecular entities in chloroform. **1** shows absorption bands at 286 nm, and 407 nm, and strong fluorescence emission at 535 nm, while **2** shows an absorption bands at 350 nm and 507 nm and strong emission at 640 nm when homogenously dissolved in chloroform.

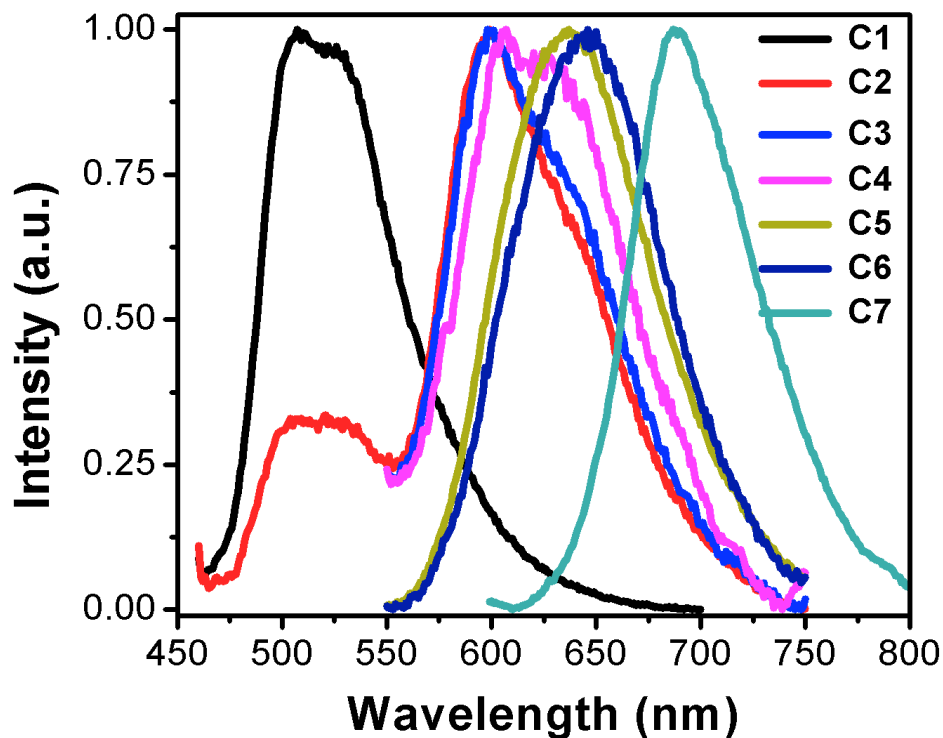


**Figure S11.** Fluorescence emission from the different co-assembled structures of **1** and **2** at various compositions. Regardless of the excitation wavelength chosen, the emission is tuned progressively as a function of composition. Pure components of **1** and **2** show strong emission at 514 and 686 nm, respectively and the emission from all the other components lies in between. In the main manuscript, select plots (**Figure 2A**) are shown for clarity.

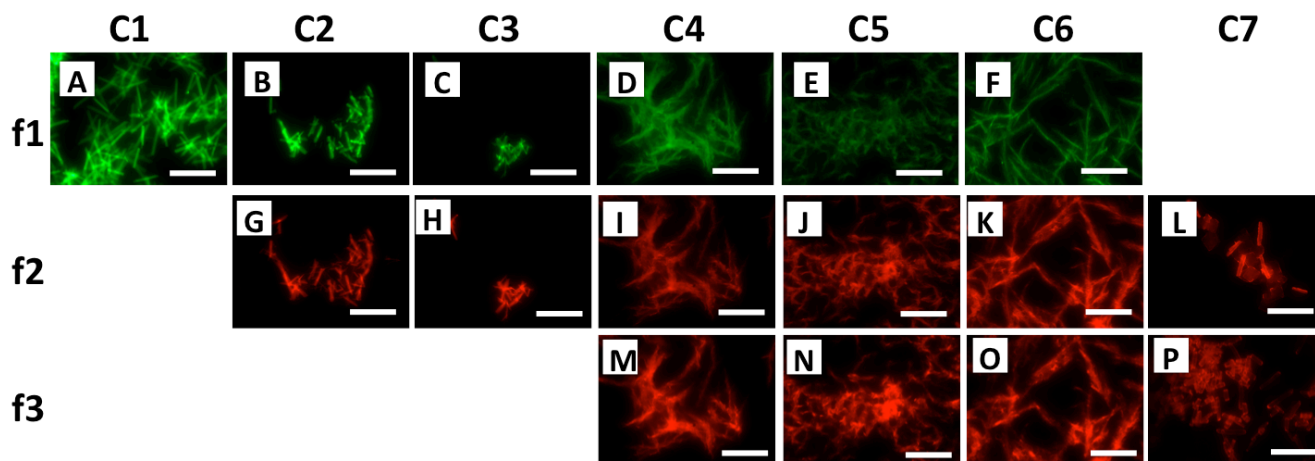


**Figure S12. (A-P)** The fluorescence emission observed for each of the compositional specific assembly under different fluorescence filter cubes. The scale bar in each case is 50  $\mu\text{m}$ . The filter cube **f1** allows for imaging regions associated with emission of **1**, while **f2** and **f3** allow for identification of **2** and emission from co-assembled structures (compositions **C2-C6**).

### Supporting Information Reference

(1) (a) Kato, S.-i.; Matsumoto, T.; Ishi-i, T.; Thiemann, T.; Shigeiwa, M.; Gorohmaru, H.; Maeda, S.; Yamashita, Y.; Mataka, S. *Chem. Commun.* **2004**, 2342; (b) Kato, S.-i.; Matsumoto, T.; Shigeiwa, M.; Gorohmaru, H.; Maeda, S.; Ishi-i, T.; Mataka, S. *Chem. Eur. J.* **2006**, *12*, 2303; (c) Zhang, X.; Gorohmaru, H.; Kadowaki, M.; Kobayashi, T.; Ishi-i, T.; Thiemann, T.; Mataka, S. *J. Mater. Chem.* **2004**, *14*, 1901; (d) Zhang, X.; Yamaguchi, R.; Moriyama, K.; Kadowaki, M.; Kobayashi, T.; Ishi-i, T.; Thiemann, T.; Mataka, S. *J. Mater. Chem.* **2006**, *16*, 736.